



**HAL**  
open science

## **Te<sub>3</sub>O<sub>5</sub>F<sub>2</sub>: a new metastable tellurium IV oxyfluoride with an acentric complex structure**

Jean-Paul Laval, Nefla Jennene-Boukharrata, Philippe Thomas

► **To cite this version:**

Jean-Paul Laval, Nefla Jennene-Boukharrata, Philippe Thomas. Te<sub>3</sub>O<sub>5</sub>F<sub>2</sub>: a new metastable tellurium IV oxyfluoride with an acentric complex structure. *Journal of Fluorine Chemistry*, 2022, 259-260, pp.109991. 10.1016/j.jfluchem.2022.109991 . hal-04767515

**HAL Id: hal-04767515**

**<https://unilim.hal.science/hal-04767515v1>**

Submitted on 13 Nov 2024

**HAL** is a multi-disciplinary open access archive for the deposit and dissemination of scientific research documents, whether they are published or not. The documents may come from teaching and research institutions in France or abroad, or from public or private research centers.

L'archive ouverte pluridisciplinaire **HAL**, est destinée au dépôt et à la diffusion de documents scientifiques de niveau recherche, publiés ou non, émanant des établissements d'enseignement et de recherche français ou étrangers, des laboratoires publics ou privés.



Distributed under a Creative Commons Attribution - NonCommercial 4.0 International License

## **Te<sub>3</sub>O<sub>5</sub>F<sub>2</sub>: a new metastable tellurium IV oxyfluoride with an acentric complex structure**

Jean-Paul Laval\*, N. Jennene-Boukharrata and Philippe Thomas

Centre Européen de la Céramique, IRCER, UMR-CNRS 7315, Université de Limoges, Faculté des Sciences,  
12 rue Atlantis, 87068 Limoges, France.

corresponding author : **Jean-Paul Laval** mail : jean-paul.laval@unilim.fr tel : +33 (0)5 55 39 27 14

### **Abstract**

The crystal structure of a new metastable tellurium (IV) oxyfluoride Te<sub>3</sub>O<sub>5</sub>F<sub>2</sub> [non-centrosymmetric P2<sub>1</sub> space group] is unusually complex with 15 different Te polyhedra. It is built of giant cylindrical columns of oxide units connected via weak Te-F bonds. A strict O/F order is evidenced and a structural comparison with Sb<sub>3</sub>O<sub>2</sub>F<sub>5</sub> shows that these two phases derive, by a different mechanism, from the anion-excess fluorite superstructure type. Surprisingly, in these two structures is observed a full gradation of various polyhedra of tellurium (IV) or antimony (III) with the oxygen atom ensuring a strong framework at the centre of these structures (cylinders for Te phase and layers for Sb one), and more and more F anions moved away at the periphery of these strong units, connecting these units *via* weak Te-F or Sb-F bonds. This well illustrates the different roles played by oxygen and fluorine atoms in the oxyfluorides of cations presenting an electronic lone pair E (5s<sup>2</sup> in the case of Te<sup>4+</sup> cation), in relation with the non-linear properties of these phases.

**Keywords:** tellurium IV oxyfluoride, crystal structure, anionic ordering, electronic lone pair.

---

## 1. Introduction:

The investigation by thermal analysis and X-ray diffraction techniques within the  $\text{TeO}_2\text{--TeF}_4$  system [1] had allowed to establish the phase diagram of this system, to isolate an extended glass domain (0.25-0.83 mole%  $\text{TeF}_4$ ) with a vitreous transition temperature  $T_g$  varying from about  $180^\circ\text{C}$  to  $-20^\circ\text{C}$  and to characterize two crystalline  $\text{Te}^{\text{IV}}$  oxidefluorides with the respective formulae  $\text{TeOF}_2$  [2] and  $\text{Te}_2\text{O}_3\text{F}_2$  [3] with original structure types.  $\text{Te}_2\text{O}_3\text{F}_2$  crystallizes with the triclinic symmetry (P-1 space group) and  $\text{TeOF}_2$  with the monoclinic  $\text{P2}_1$  acentric space group. The bond valence calculations show a perfect O/F order and a stereochemical activity of the lone pair E of the  $\text{Te}^{4+}$  cations is in both structures. In  $\text{Te}_2\text{O}_3\text{F}_2$   $\text{Te}_2\text{O}_4\text{F}_2\text{E}$ , bipolyhedral units constitute by sharing O corners, independent twisted sheets, similar to those described in  $\beta\text{-TeO}_2$ . In  $\text{TeOF}_2$ , quasi-independent helical chains of  $\text{TeO}_2\text{F}_3\text{E}$  polyhedra share O corners. All the F atoms are non-bridging and orientated, together with the E lone pairs, toward the interlayer space. A structural relationship of  $\text{Te}_2\text{O}_3\text{F}_2$  with the  $\beta\text{-TeO}_2$  structure and of  $\text{TeOF}_2$  with the  $\alpha\text{-TeO}_2$  structure has been established.

The present paper deals with the synthesis and the structural determination on single crystal of a third metastable oxyfluoride  $\text{Te}_3\text{O}_5\text{F}_2$ , unknown until now and closer to Te dioxide, this last oxide being the basis of many phases of great interest for their non-linear optical properties. Oxyhalides of cations presenting a stereoactive electronic lone pair are also the subject of a great interest in the same field.

The acentric structure of  $\text{Te}_3\text{O}_5\text{F}_2$  is unusually complex and has unique features, related to a long range O/F order. It is compared to other complex phases comprising a cation with an electronic lone pair E.

## 2. Experimental

---

A small number of single crystals in shape of small cleaved rods were obtained randomly as a by-product in the pseudo-binary  $\text{InF}_3\text{-TeO}_2$  for compositions close to  $\text{InF}_3\text{-3TeO}_2$  heated about 400 °C in a Pt sealed tube and water-quenched.  $\text{InF}_3$  (Aldrich, >99.9% purity) and  $\text{TeO}_2$  (prepared in the laboratory by calcination of orthotelluric acid  $\text{H}_6\text{TeO}_6$  in a Pt container at 550°C during 1 day) were mixed in a glove box under dry  $\text{N}_2$  atmosphere. The analysis of these single crystals by EDX shows that, in fact, they don't contain indium and are likely a tellurium oxyfluoride, hypothesis confirmed by the structural study determining without ambiguity a composition  $\text{Te}_3\text{O}_5\text{F}_2$ . Attempts to synthesize this phase by solid state reaction between  $\text{Te}_2\text{O}_3\text{F}_2$  and  $\text{TeO}_2$  in Au or Pt sealed tubes about 350-400°C fail likely because of the thermal instability and the high vapor pressure of the  $\text{Te}^{\text{IV}}$  fluoride and oxyfluorides in this temperature range (see the  $\text{TeO}_2\text{-TeF}_4$  diagram [1]). Synthesis by dissolution of a Te salt in HF and recrystallisation was also unsuccessful. It is likely that these single crystals result from a chemical transport process with  $\text{InF}_3$  acting as a fluorinating agent on initial  $\text{TeO}_2$ . That explains the non-reproducibility of the reaction and the formation of only few crystals inside the Pt-sealed tubes. This new phase is likely metastable and exists in a very narrow thermal domain.

The diffraction pattern is recorded on a 4-circle P4-Siemens diffractometer equipped with a graphite monochromator and a scintillation counter using the *XSCANS* program [4]. Absorption correction by a psi-scan method uses the program *XEMP* [5]. The structure is solved by direct methods using *SHELXS-86* and refined with *SHELXL-2018/3* [6], using the *WINGX* integrator *V2018-3* [7]. The pictures are drawn using *DIAMOND* software [8].

### 3. Results and discussion

---

Although the quality of the single crystals was rather weak, we have tried to determine, as well as possible, the structure of this phase. However, if all the cationic and anionic positions and the isotropic thermal displacements are determined with enough accuracy, the anisotropy of the thermal displacements is well refined only for the cationic sites but remains slightly non-definite/negative for several anions. The examination of the diffraction spots shows that there is no clear twinning of the crystals but rather a beginning of decomposition of this metastable phase during the cooling process, in spite of a water quenching of the sealed tubes. That generates some diffuse scattering around many diffraction reflections, likely responsible of the difficulty to refine the anisotropic thermal vibration factors of the anions. However, the refined structure is perfectly logical, although very complex; all the interatomic distances are normal and the R1 factor stabilizes at 6.29% in the acentric space group  $P2_1$ , selected without any doubt with the  $|E^2-1|$  criterion = 0.745(18) (0.968 for centric, 0.736 for ideal acentric symmetry). After complete refinement, the absolute structure has to be inverted, the fractional contribution of the inverted component of a “racemic twin” (Flack parameter) being 1.09 (17) [9].

The crystal data and structural refinement data are gathered in table 1. The refined atomic coordinates in table S1, the main bond lengths in table S2 and the anisotropic thermal factors of Te in table S3 are reported as supplementary material in annexes. To confirm the validity of the refinement and determine the O/F anionic ordering, the bond valences are calculated with the program *VALIST* [10] using the Brown and Altermatt method [11, 12] and are gathered in Table 2.

Considering the difficulty of synthesis of this phase, the interest of its very original crystal structure and its potential physical properties, the main features of the crystal structure of  $Te_3O_5F_2$  are described in the present paper.

**Table 1:** Crystal data and structure refinement for  $Te_3O_5F_2$ .

Elementary formula	Te <sub>3</sub> O <sub>5</sub> F <sub>2</sub>
Formula weight	500.80 g.mol <sup>-1</sup>
Temperature	293(2) K
Wavelength	0.7107 Å
Crystal system, space group	Monoclinic, P2 <sub>1</sub>
Unit cell dimensions	a = 16.547(4) Å b = 6.360(2) Å β = 119.04(2)° c = 16.938(4) Å
Volume	1558.4(8) Å <sup>3</sup>
Z, Calculated density	10, 5.336 g/cm <sup>3</sup>
Absorption coefficient	13.953 mm <sup>-1</sup>
F(000)	2140
Crystal size	0.08 x 0.05 x 0.04 mm
Theta range for data collection	2.40 to 30.00°
Reflections collected / unique	5203 / 5171 [R(int) = 0.092]
Refinement method	Full-matrix least-squares on F <sup>2</sup>
Completeness to theta = 25.242°	58.1 %
Data / restraints / parameters	5171 / 1 / 278
Goodness-of-fit on F <sup>2</sup>	1.020
Final R indices [I>2sigma(I)]	R1 = 0.0629, wR2 = 0.1245
R indices (all data)	R1 = 0.1103, wR2 = 0.1449
Extinction coefficient	0.00028(6)
Largest diff. peak and hole	1.64 and -1.65 e.Å <sup>-3</sup>
Estimated min. and max. transmission	0.464 and 0.579

### 3.1 Description of the structure

The structure of Te<sub>3</sub>O<sub>5</sub>F<sub>2</sub> is unusually complex for a structure containing a single type of cation with a single valence. Indeed, the acentric unit cell, of space group P2<sub>1</sub> and volume V = 1558.4 Å<sup>3</sup>, includes 15 independent cationic sites, 25 O sites and 10 F sites.

**Table 2:** Bond valences of cations and anions and Te IV polyhedra in Te<sub>3</sub>O<sub>5</sub>F<sub>2</sub>, (calculated using Brown and Altermatt approach with R = 1.955 Å, B = 0.44 for Te - O bonds, R = 1.87 Å and B = 0.37 for Te - F bonds [11, 12]). The Te polyhedra incorporate weak Te-O and Te-F bonds <3.26 Å.

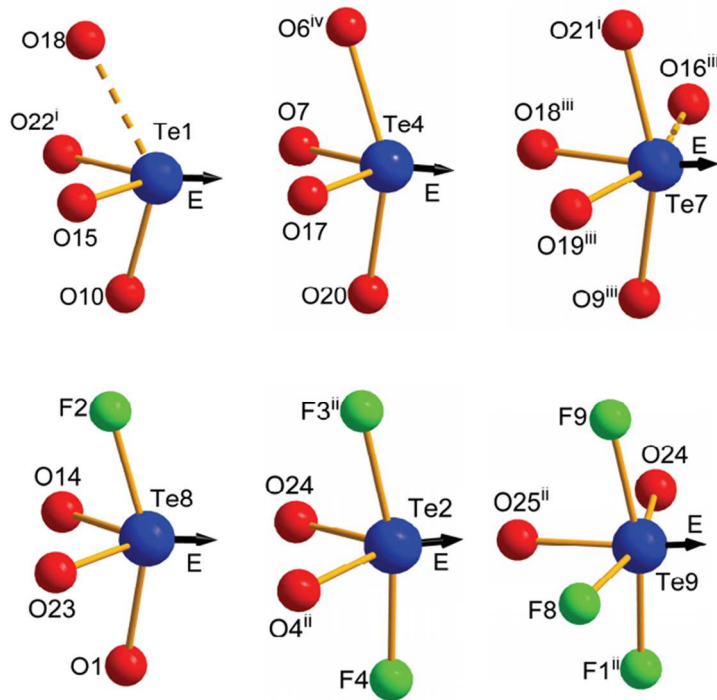
Te1	Te2	Te3	Te4	Te5	Te6	Te7	Te8	Te9	Te10
3.86	4.03	3.98	3.99	3.93	4.08	4.08	3.92	4.05	4.00
TeO <sub>3+3</sub> F	TeO <sub>2</sub> F <sub>2+2</sub>	TeO <sub>4+3</sub>	TeO <sub>4+2</sub> F <sub>0+1</sub>	TeO <sub>3+3</sub> F <sub>0+2</sub>	TeO <sub>4+4</sub>	TeO <sub>4+2</sub>	TeO <sub>3+3</sub> F <sub>1+1</sub>	TeO <sub>2</sub> F <sub>3+1</sub>	TeO <sub>3+3</sub> F <sub>0+1</sub>
Te11	Te12	Te13	Te14	Te15	O1	O2	O3	O4	O5

---

3.91	4.02	3.88	3.77	4.24	2.23	2.26	2.01	2.11	1.95
TeO <sub>2</sub> F <sub>3+2</sub>	TeO <sub>3+1</sub> F <sub>1+2</sub>	TeO <sub>3+3</sub> F <sub>0+1</sub>	TeO <sub>4</sub> F <sub>0+3</sub>	TeO <sub>4+3</sub> F <sub>0+1</sub>					
<b>O6</b>	<b>O7</b>	<b>O8</b>	<b>O9</b>	<b>O10</b>	<b>O11</b>	<b>O12</b>	<b>O13</b>	<b>O14</b>	<b>O15</b>
2.06	2.16	1.92	2.04	2.21	2.05	2.26	2.14	1.99	2.13
<b>O16</b>	<b>O17</b>	<b>O18</b>	<b>O19</b>	<b>O20</b>	<b>O21</b>	<b>O22</b>	<b>O23</b>	<b>O24</b>	<b>O25</b>
1.74	1.97	1.96	2.00	1.98	1.91	2.31	1.94	2.19	2.18
<b>F1</b>	<b>F2</b>	<b>F3</b>	<b>F4</b>	<b>F5</b>	<b>F6</b>	<b>F7</b>	<b>F8</b>	<b>F9</b>	<b>F10</b>
0.89	0.73	0.82	0.77	0.79	0.79	0.91	0.89	0.77	0.71

By limiting the distances Te - O and Te - F to 2.3 Å, classical polyhedra TeO<sub>3</sub>, TeO<sub>4</sub>, TeO<sub>3</sub>F, TeO<sub>2</sub>F<sub>2</sub> and TeO<sub>2</sub>F<sub>3</sub> are described, as some examples shown on Fig. 1, but the bond valences calculated on this basis are often far from the real charge of the cations and anions. A second calculation, performed in adding the Te - O and Te - F weaker bonds between 2.2 and 3.26 Å, gives much better calculated bond valences and confirms that all the Te cations have a +4 charge and true coordination numbers ranging from 6 and 8, as reported in Table 2. The bond valences, calculated for the anions and reported in the same Table, show a perfect O / F anionic order in this structure and confirm the reasonable accuracy of the refined anionic positions, in spite of the limited quality of the single crystal.

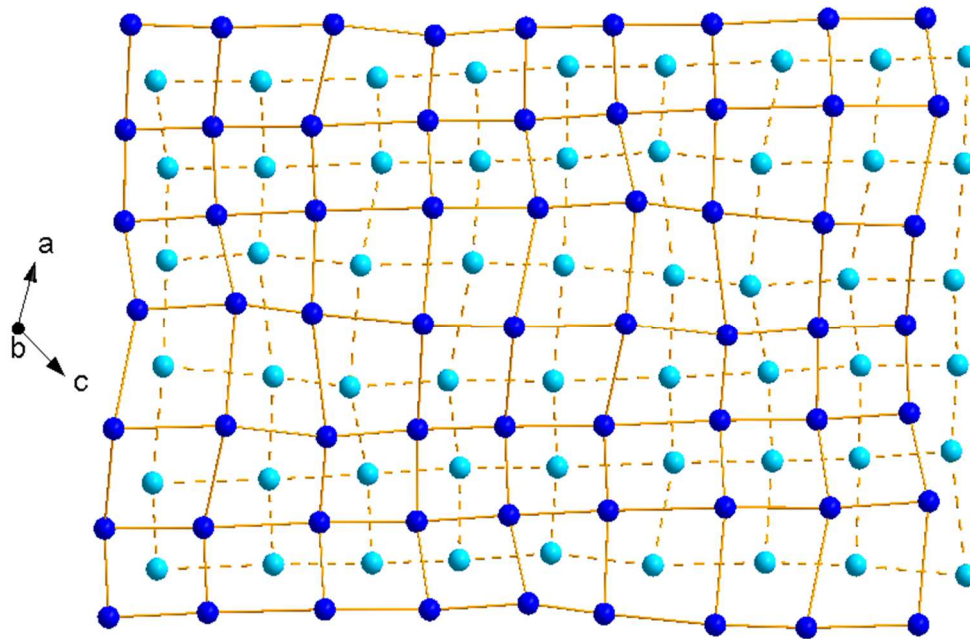
**Fig. 1:** Main classical polyhedra of Te<sup>4+</sup> (with Te - O and Te - F <2.45 Å). The electronic E lone pair of Te<sup>4+</sup> is represented by an arrow.



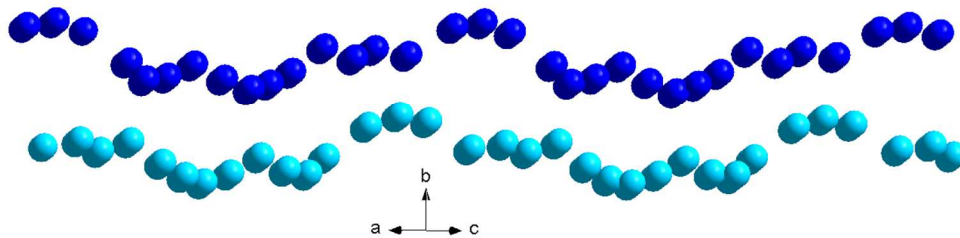
The network of tellurium atoms derives from a face-centered cubic lattice (*fcc*) rather distorted and quite wavy (Figs. 2a and b).

**Fig. 2:** **a:** projection along  $[010]$  showing the cationic very distorted *fcc* fluorite network of  $\text{Te}_3\text{O}_5\text{F}_2$ . dark blue = Te at  $y_{\text{av.}} \sim 0.20$  (0.05-0.41); light blue = Te at  $y_{\text{av.}} \sim 0.70$  (0.55-0.91). **b:** view along  $[101]$  axis, showing the wavy plane nets of Te cations: the most distorted parts correspond to the cations mainly connected to F anions and located at the boundaries between adjacent cylindrical columns.





a



b

This network includes, in its most regular part, very short Te - Te distances when the cations are connected *via* O - O edges, for example Te12 - Te4 = 3.172 Å (as in the Te<sub>2</sub>O<sub>6</sub> units of α-TeO<sub>2</sub>) or Te10 - Te8 = 3.379 Å. When the connections operate through O - O common vertices, these distances Te - Te are logically longer and range between about 3.6 and 4 Å. Finally, much longer Te - Te distances (4.4 to 5.5 Å) correspond to cations only connected *via* very weak Te - F bonds (2.64 ≤ Te - F ≤ 3.3 Å).

It can therefore be distinguished a "strong" network corresponding to quasi-cylindrical columns as shown in the projection of fig. 3, with their central part consisting only of tellurium atoms and oxygen atoms and intercationic connections mainly ensured *via* O–O edges. Each column includes a group of 15 tellurium atoms indefinitely repeated along the [0 1 0] axis of the column.

**Fig. 3:** Projection onto the (010) plane of a right non-circular cylindrical column of Te IV cations only interconnected *via* O anions, forming a strong network. All the F peripheral anions are connected *via* weak Te-F bonds with the adjacent cylindrical units.

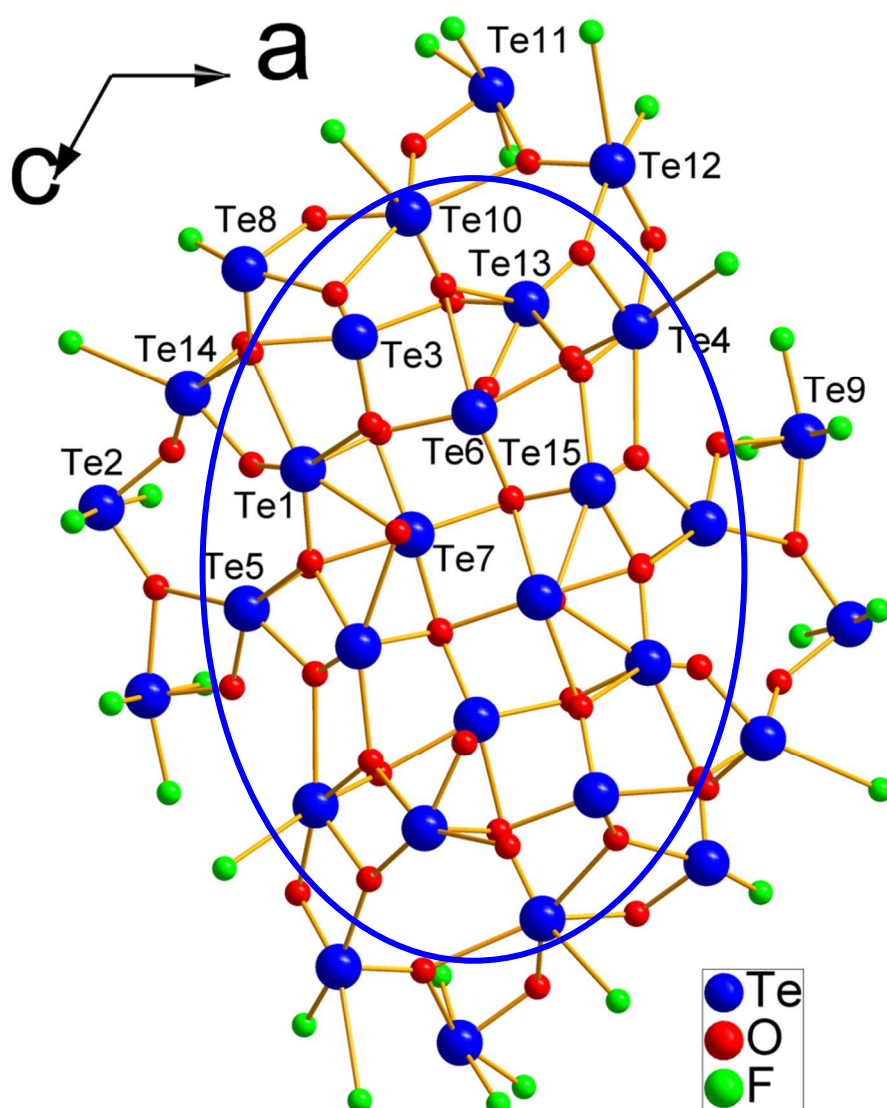
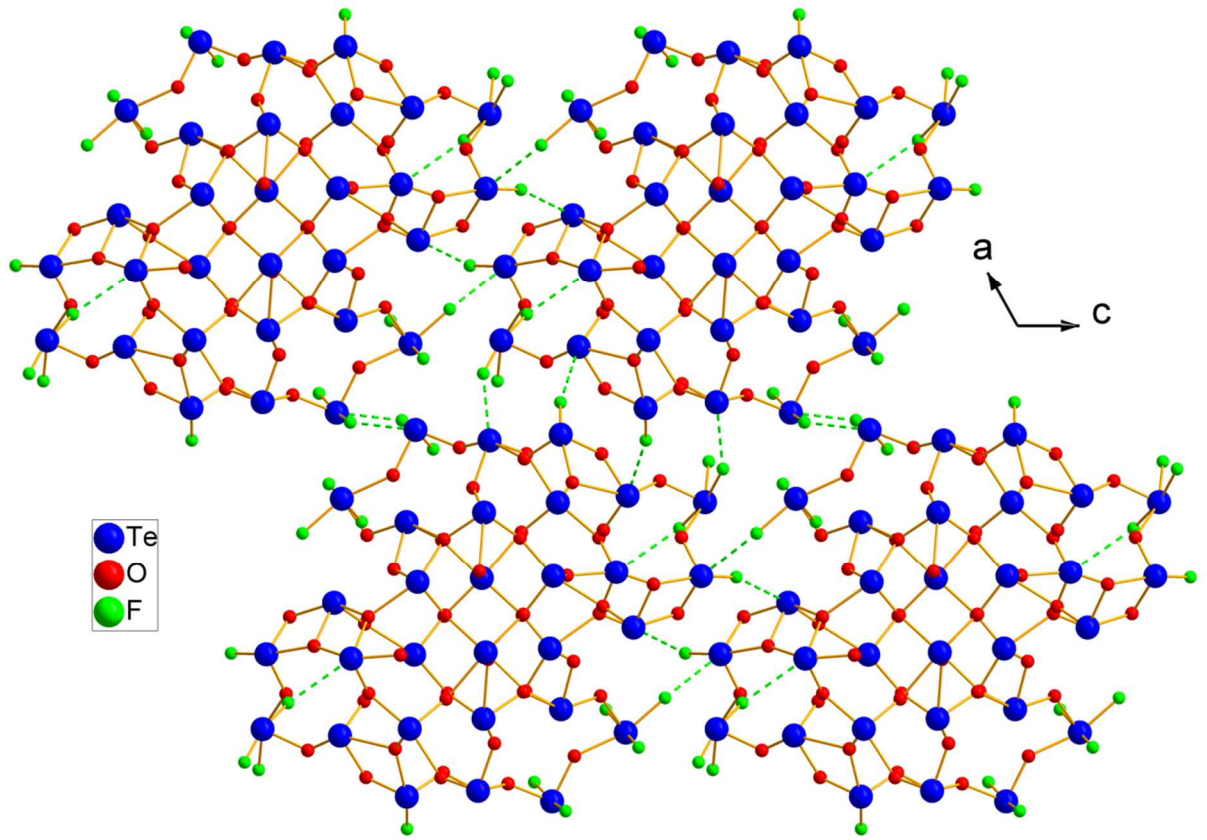


**Fig. 4:** Projection onto the (010) plane of the pseudo-hexagonal distribution of the cylindrical strong units of fig. 3, showing their interconnection *via* weak Te - F bonds ( $2.64 \text{ \AA} \leq \text{Te} - \text{F} \leq 2.9 \text{ \AA}$ ) represented by dotted lines.



---

The peripheral part of the columns, made up of oxyfluorinated polyhedra, is much more relaxed: all F<sup>-</sup> anions, located in "quasi-terminal" positions, that is to say linked only to one Te<sup>4+</sup> atom by a very short bond (~1.9 Å), are repelled to the periphery, in contact with the "intercolumnar" space. These "terminal" F<sup>-</sup> anions also ensure, by very weak Te - F bonds the cohesion with the contiguous cylindrical columns. The Figure 4 represents by dotted lines the weak bonds Te - F <2.9 Å which mainly interconnect the strong cylindrical columns. Another series of very weak connections (3 Å <Te - F <3.3 Å) operates secondarily. The structure of each cylindrical column can therefore be considered almost independently of the others and their packing is almost hexagonal, in agreement with the monoclinic unit cell which derives from hexagonal symmetry with  $a \sim c = a_{\text{hex}}$ ,  $b = c_{\text{hex}}$  and  $\beta = \gamma_{\text{hex}} \sim 119^\circ$ .

However, examination of the fig. 2a also shows that the *fcc* cationic network is not completely broken at the level of the intercolumnar space and that its continuity is ensured between adjacent columns.

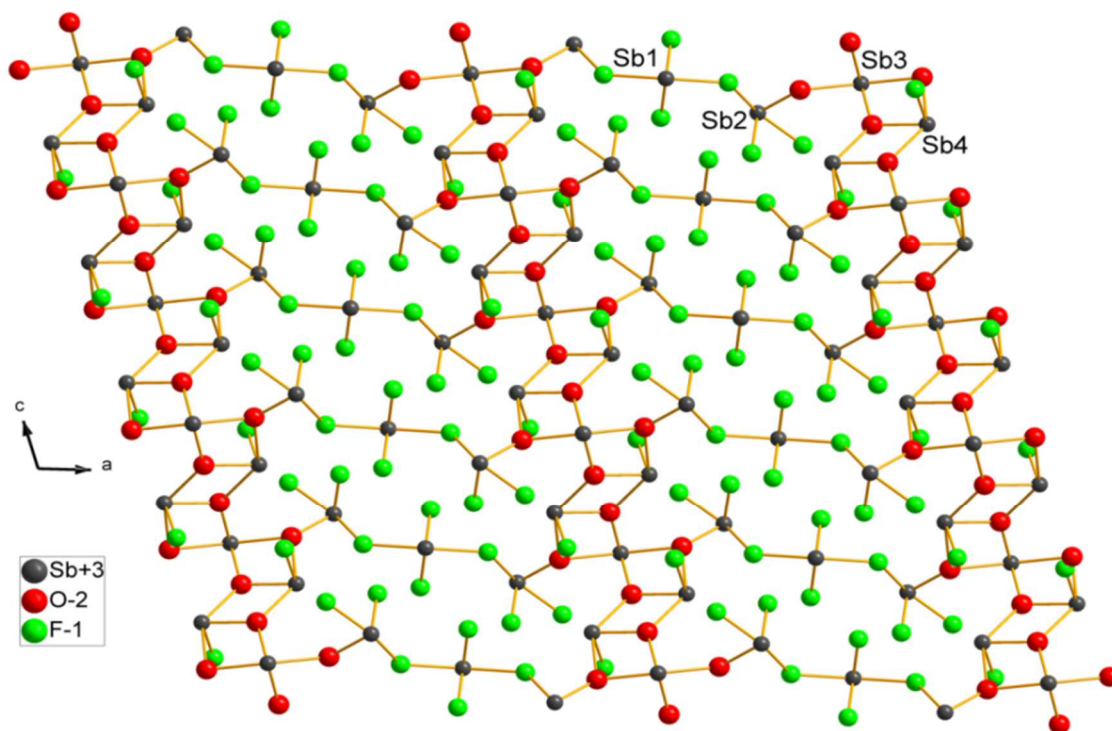
The segregation of the anions O and F with two quite distinct roles constitutes the main feature of the O / F order in this oxyfluoride and partially explains the complexity of this structural type. It can also be noted that a large part of the anions O is located in the tetrahedral sites of this network, site occupied by the anions in the fluorite structure. This last point will be developed in a next paragraph.

### **3.2 Comparison with other complex phases comprising a cation with an electronic lone pair E:**

Few oxyfluorinated, fluorinated or oxide phases based on a single cation as complex as Te<sub>3</sub>O<sub>5</sub>F<sub>2</sub> have been described. The main one that can be compared is Sb<sub>3</sub>O<sub>2</sub>F<sub>5</sub> [13-15], isoformulary with an inversion of the relative proportions of oxygen and fluorine.

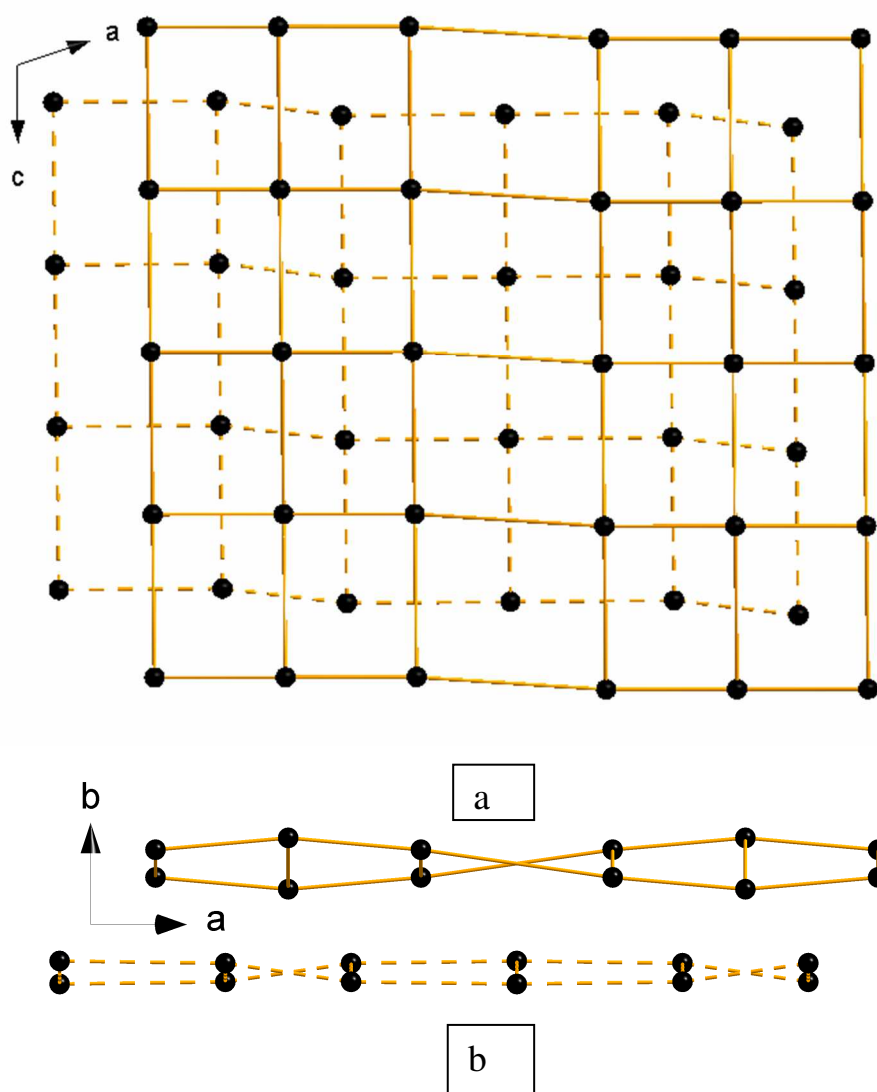
The  $\text{Sb}_3\text{O}_2\text{F}_5$  phase has only four Sb, five F and two O sites. Unlike  $\text{Te}_3\text{O}_5\text{F}_2$ ,  $\text{Sb}_3\text{O}_2\text{F}_5$  is centrosymmetric with space group  $P 2 / c$  and a much lower cell volume ( $679 \text{ \AA}^3$  against  $1558 \text{ \AA}^3$  for  $\text{Te}_3\text{O}_5\text{F}_2$ ). In this structure, the anionic order is also established in a very particular way: it can be observed along the direction  $[1 0 0]$  a successive transition from purely fluorinated layers, composed of  $\text{SbF}_4$  polyhedra, to purely oxygenated layers composed of  $\text{SbO}_4$  polyhedra, *via* layers of mixed  $\text{SbOF}_3$  and  $\text{SbO}_3\text{F}$  polyhedra (Fig. 5). As also in  $\text{Te}_3\text{O}_5\text{F}_2$  (Table 2), Ali and Johnsson [14] show by BVS calculations for the Sb oxyfluorides, a slight hypervalence in a strong Sb and O framework and a slight hypovalence in the Sb - F framework.

**Fig. 5:** Projection onto (010) plane of the  $\text{Sb}_3\text{O}_2\text{F}_5$  structure.



As in  $\text{Te}_3\text{O}_5\text{F}_2$ , the cationic framework in  $\text{Sb}_3\text{O}_2\text{F}_5$  (Fig. 6) derives from a distorted and wavy *fcc* lattice, comprising shorter Sb – Sb distances in the most oxygenated layers (Sb – Sb = 3.35 and 3.95 Å) and looser connections in the purely fluorinated layers (Sb – Sb = 3.68; 4.05; 4.22 and 4.64 Å).

**Fig. 6:** **a:** Sb double cationic layer in  $\text{Sb}_3\text{O}_2\text{F}_5$ , homologous of Figs. 2 a and b of  $\text{Te}_3\text{O}_5\text{F}_2$ . **b:** view along (011) plane of the Sb wavy cationic layers of  $\text{Sb}_3\text{O}_2\text{F}_5$ .



It can be observed in the two structures a modulation of the O / F order between two extreme areas, fully oxygenated and fully or partially fluorinated, preserving in both cases the distorted *fcc* cationic network. The main difference consists in the formation in

---

$\text{Te}_3\text{O}_5\text{F}_2$  of "oxide" zones of cylindrical shape, separated by fluorinated side walls and in  $\text{Sb}_3\text{O}_2\text{F}_5$  of successive "oxide" and "fluoride" layers and therefore of an O / F order in two-dimensional sheets.

Most of the oxyfluorides of cations presenting a stereoactive electronic lone pair E also have a strict anionic order: in the two varieties of SbOF, L [16] and M [17], the  $\text{SbO}_3\text{F}$  units constitute, by pooling of O-O edges, respectively chains and folded layers. The two types of anions play a different role: the oxygen atoms provide the strong connections within layers or chains and the fluorine atoms are essentially quasi-terminal anions, nevertheless ensuring weak inter-chain connections ( $\text{Sb-F} = 2.8$  to  $3.2 \text{ \AA}$ ) as also observed in  $\text{TeOF}_2$  [2].

A strict anionic order also exists in BiOF [18],  $\text{Sn}_2\text{OF}_2$  [19] and  $\text{Sn}_4\text{OF}_6$  [20]. Oxyfluorides having a molecular character such as  $\text{SeOF}_2$  [21] and  $\text{XeO}_2\text{F}_2$  [22] also exhibit a strict O / F order with M - O bonds significantly stronger than M - F bonds. Brown [23], studying the characteristics of the  $\text{MX}_3\text{E}$ ,  $\text{MX}_4\text{E}$  and  $\text{MX}_5\text{E}$  polyhedra in oxides and mixed oxyfluorides of Sn II, Sb III, Te IV, I V and Xe VI, already distinguished three kinds of bonds, resp. strong, intermediate and weak, e. g. in  $\text{TeF}_4$ . He noticed that oxygen preferably occupies, e. g. in  $\text{IOF}_4^-$ , the apical position strongly linked to  $\text{I}^{5+}$  and observed in  $\text{KXeO}_3\text{F}$  [24] the presence of three Xe-O bonds forming a strong unit  $\text{XeO}_3$ , the F anions providing, through moderately weak bonds, a bridging between these strong units to form an infinite polyion:  $-\text{[F} - \text{XeO}_3 - \text{F}' - \text{XeO}_3 - \text{F}] -$ . In summary, in the oxyfluorides of elements with an unengaged electronic pair, there is usually a strict O / F order, especially when these anions are likely to play a different structural role, depending on their charge. This is the case in the major part of these phases which include, through the formation of strong units (layers or chains) resulting from the spatial distribution of the lone pairs E, a well-structured strong part and a looser peripheral part. Quite naturally, the



---

oxygen atoms provide the strong central bonds and fluorine atoms the weaker peripheral bonds.

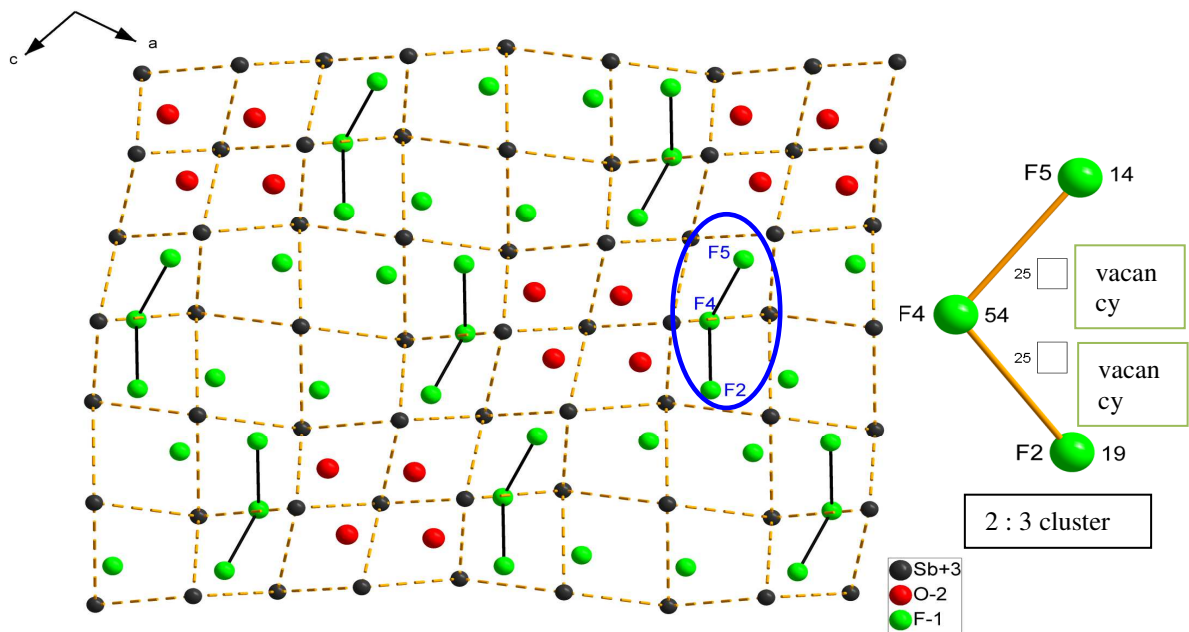
### 3.3 Comparison with fluorite structure:

If one consider that fluorite structure has a cationic *fcc* network,  $\text{Sb}_3\text{O}_2\text{F}_5$  and  $\text{Te}_3\text{O}_5\text{F}_2$  are also in this case. A second characteristic of the cubic Fm-3m fluorite structure  $\text{CaF}_2$  or  $\text{UO}_2$  is the occupancy by the F or O anions of the anionic site ( $\frac{1}{4}, \frac{1}{4}, \frac{1}{4}$ ) with each anion located at the centre of a tetrahedron of cations at (0, 0, 0). The two lattices of  $\text{Te}_3\text{O}_5\text{F}_2$  and  $\text{Sb}_3\text{O}_2\text{F}_5$  comprise a parameter  $b$  homologous to that of fluorite ( $b = 6.360$  and  $5.927 \text{ \AA}$  respectively against  $5.462 \text{ \AA}$  for  $\text{CaF}_2$ ) with cations forming a distorted *fcc*-type network developed in the (0 1 0) plane of the two structures. The  $\text{Te}^{4+}$  and  $\text{Sb}^{3+}$  cations are located in parallel layers homologous to the fluorite cationic layers with  $y = \frac{1}{2}$  and 0 and a large part of the anions is located inside the tetrahedron formed by four adjacent cations at  $y \sim \frac{1}{4}$  and  $\frac{3}{4}$ . However, due to the stereochemical activity of the electronic lone pair E of these cations, the anions systematically move away from the centre of these tetrahedra and the coordination [8] of these cations in the ideal fluorite structure is reduced to [4] or [6] strong or intermediate Te(Sb) – O and Te(Sb) – F bonds but completed to [6] [7] or [8] by incorporating weak Te(Sb) – O and Te(Sb) – F bonds.

It can be noticed in the structure of  $\text{Sb}_3\text{O}_2\text{F}_5$  (Fig. 7) the presence of groups of four  $\text{O}^{2-}$  and four  $\text{F}^-$  anions in normal anionic site (sometimes very shifted) and three anions F5, F2 and F4 respectively occupying the inner of two contiguous Sb tetrahedra. This last arrangement is reminiscent of an anion-excess fluorite-type structure.

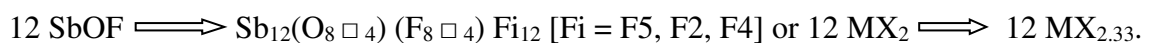
**Fig. 7:** Projection onto the (010) plane of the structure of  $\text{Sb}_3\text{O}_2\text{F}_5$  showing its relationship with anion-excess fluorite structure family by formation of 2 : 3 anionic clusters (2 vacancies and 3  $\text{F}_i$  interstitials, in Willis notation).





This generic type of structure actually covers several different mechanisms of accommodation of the anionic excess, transforming an ideal  $\text{MX}_2$  fluorite to an anion-excess phase, as e.g. other  $\text{MX}_{2.33}$  phases  $\text{Ca}_2\text{LnF}_7$  [25],  $\text{Pb}_2\text{InF}_7$ , [26],  $\text{Sr}_2\text{RhF}_7$  [27],  $\text{U}_3\text{O}_7$  [28].

In  $\text{Sb}_3\text{O}_2\text{F}_5$ , it can be proposed a mechanism such as two anions in normal site are replaced by three interstitial anions according to the following diagram:



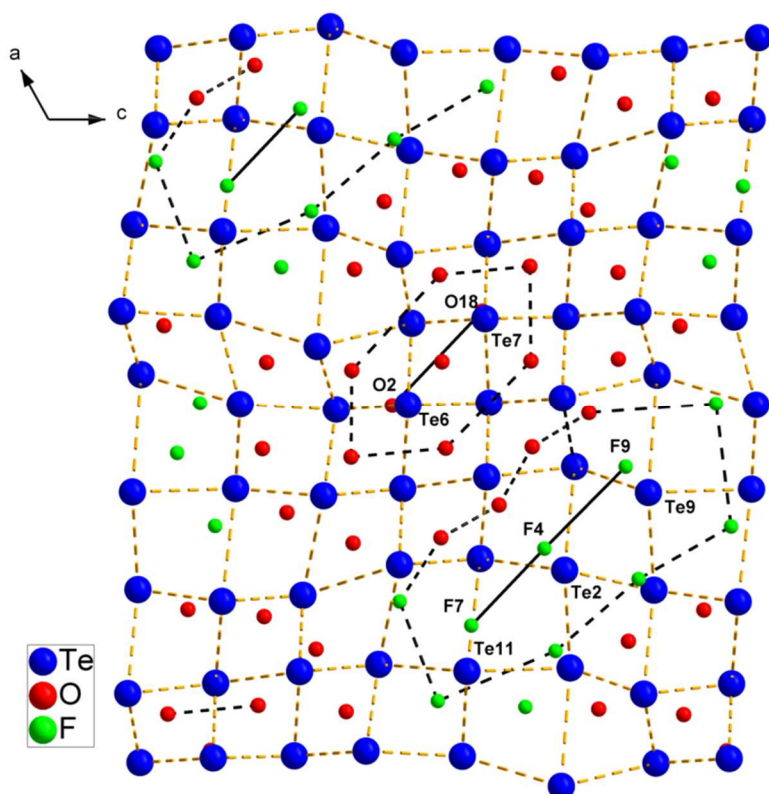
This simple mechanism explains the anionic excess leading from a composition  $\text{MX}_2$  to  $\text{MX}_{2.33}$ .

Using Willis notation, the defect (or "anionic cluster") allowing to accommodate the anionic excess can be called **2:3** (2 anion vacancies, 3 interstitials  $\text{F}_i$ ). The distortion of the fluorite network, inherent in the phases comprising a cation with an electronic lone pair E, does not make it possible to really distinguish one of the two types of interstitials  $\text{F}'$  or  $\text{F}''$  defined by Willis [29].

The defect highlighted in  $\text{Sb}_3\text{O}_2\text{F}_5$  is similar to the homologous defect described in  $\text{Lu}_3\text{O}_2\text{F}_5$  [30] which is the basis of the series of ordered anion-excess fluorite phases

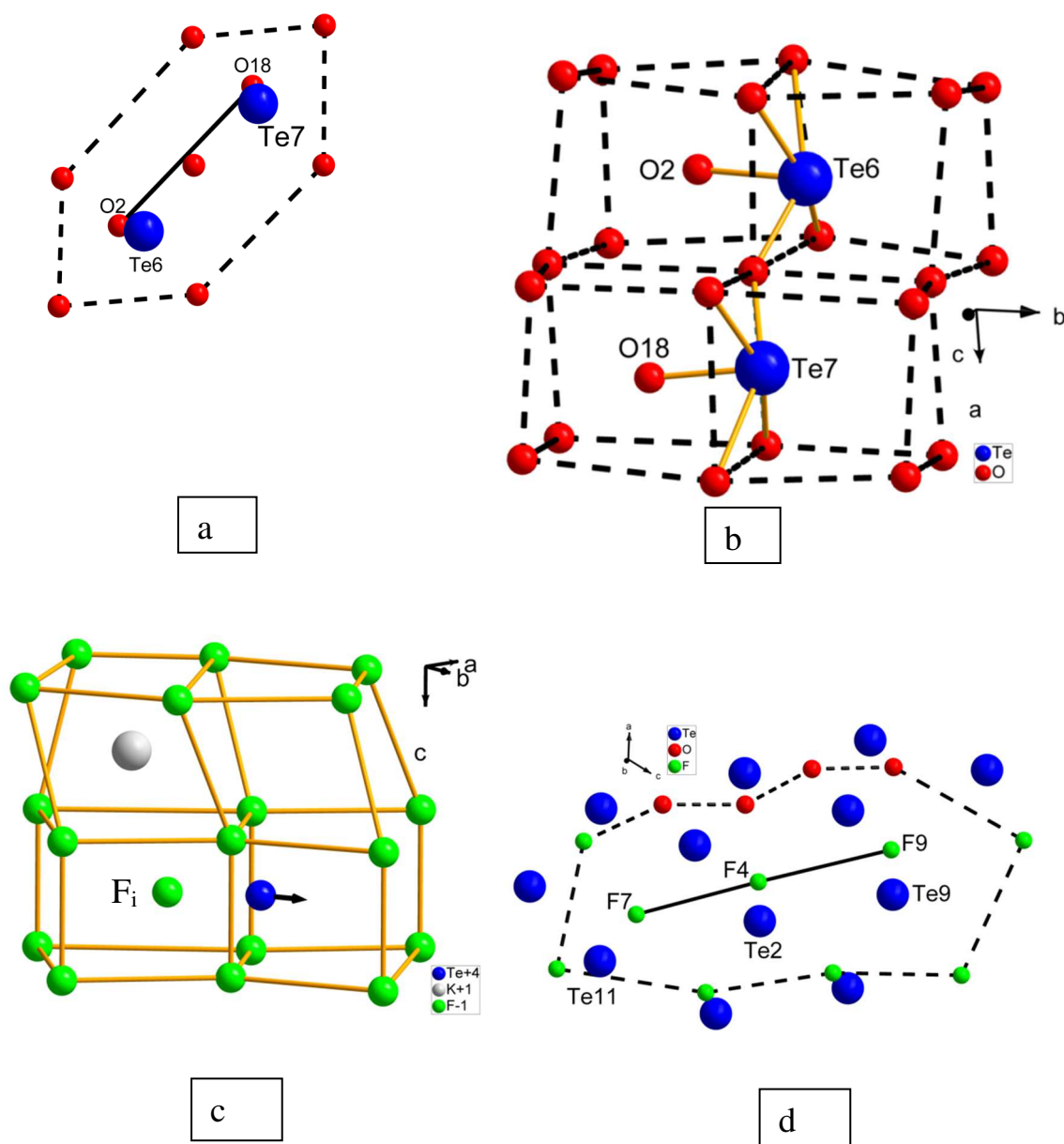
$M_nX_{2n+1}$  called "vernier" phases or "infinitely adaptable" phases in which the local densification due to the insertion of the anionic excess in (2: 3) clusters is "absorbed" by a progressive shift of the adjacent anionic rows, according to the principle of the "vernier" effect [31, 32]. In  $\text{Lu}_3\text{O}_2\text{F}_5$  also, the F sub-network is the only one concerned by the densification but the strict O / F order, different from that described in  $\text{Sb}_3\text{O}_2\text{F}_5$ , plays an important role in the stabilization of the structure (Fig. 8). However, the structure of  $\text{Lu}_3\text{O}_2\text{F}_5$  is closer to a classical fluorite structure than that of  $\text{Sb}_3\text{O}_2\text{F}_5$  and *a fortiori* that of  $\text{Te}_3\text{O}_5\text{F}_2$  due, as already noticed, to the distortion resulting from the stereochemical influence of the electronic lone pair E of  $\text{Sb}^{3+}$  and  $\text{Te}^{4+}$ .

**Fig. 8:** Projection onto (010) plane of the structure of  $\text{Te}_3\text{O}_5\text{F}_2$  showing its relationship with anion-excess fluorite structure family.



In  $\text{Te}_3\text{O}_5\text{F}_2$ , the  $\text{O}^{2-}$  anions mainly occupy the tetrahedral anionic fluorite site, with much more pronounced displacements than in  $\text{Sb}_3\text{O}_2\text{F}_5$ , by reference to the fluorite structure (Fig. 8). The defect structure is much more complex; two different types of anionic clusters can be described:

**Fig. 9:** Comparison between the defect affecting O anions around Te6 and Te7 cations in  $\text{Te}_3\text{O}_5\text{F}_2$  (**a:** and **b:**) and affecting F anions around Te in the anion-excess fluorite  $\text{KTeF}_5$  (**c:**); F cluster in  $\text{Te}_3\text{O}_5\text{F}_2$  (**d:**).



---

-The first only affects the oxygen network at the centre of each cylindrical unit defined above (around atoms Te6 and Te7) (Fig. 9a). It corresponds to the formation of two neighbouring polyhedra  $\text{TeO}_5$  linked by vertex to form a bipolyhedron  $\text{Te}_2\text{O}_9$  (Fig. 9b). This arrangement reminds the structure of  $\text{KTeF}_5$  [33] in which a  $\text{TeF}_5\text{E}$  polyhedron is described. This polyhedron derives from a  $\text{TeF}_8$  cube with an additional anion occupying the centre of a neighbouring cubic vacancy (Fig. 9c).

-The second affects the "intercolumnar" fluorinated network (around the atoms Te11, Te2 and Te9). It consists of three interstitial anions (F7, F4, F9) lined up at the same y coordinate (Fig. 9d). These  $\text{F}_i$  anions repel all the concentric O and F anions from their normal site.

#### 4. Conclusion:

In the system  $\text{TeO}_2$ - $\text{TeF}_4$  system, a new metastable tellurium (IV) oxyfluoride  $\text{Te}_3\text{O}_5\text{F}_2$  is structurally characterized in spite of the weak quality of the single crystals. Its structure, unusually complex with 15 different Te polyhedra, is built of giant cylindrical columns of oxide units interconnected *via* weak Te-F bonds. A strict O / F order is evidenced and a structural comparison with  $\text{Sb}_3\text{O}_2\text{F}_5$  shows that these two phases derive, by a different mechanism, from the anion-excess fluorite superstructure type. Interestingly, in both structures is observed a full gradation of various polyhedra of antimony or tellurium from purely oxide to oxyfluoride and / or purely fluoride polyhedra. The oxygen atoms ensure a strong framework at the centre of these structures and the fluorine atoms are pushed back at the periphery forming loose connections between adjacent strong units or even in "terminal" position in the "intercolumnar" space, that is to say linked only to one  $\text{Te}^{4+}$  cation. This illustrates well the different roles of oxygen and fluorine atoms in these ordered oxyfluorides.

---

## References

- [1] A. Ider, J.P. Laval, J. Carré, J.P. Bastide, B. Frit, « Etude du système  $\text{TeO}_2\text{-TeF}_4$ . Caractérisation structurale et thermique », *Thermochim. Acta* 258 (1995) 117-124.
- [2] L. Guillet, A. Ider, J.P. Laval, B. Frit, « Crystal Structure of  $\text{TeOF}_2$  », *J. Fluorine Chem.* 93(1) (1999) 33-38.
- [3] A. Ider, J.P. Laval, B. Frit, J. Carré, J.P. Bastide, « Crystal Structure of  $\text{Te}_2\text{O}_3\text{F}_2$  », *J. Solid State Chem.* 123(1) (1996) 68-72.
- [4] XSCANS, XPREP, Siemens Analytical X-ray instruments Inc., Karlsruhe, Germany.
- [5] G.M. Sheldrick, (1993) XEMP, SHELXTL-PC, Siemens Analytical X-ray instruments Inc., Karlsruhe, Germany.
- [6] G.M. Sheldrick, « Crystal structure refinement with Shelxl », *Acta Crystallogr.* C71 (2015) 3-8.
- [7] L.J. Farrugia, « *WinGX* and *ORTEP for Windows*: an update », *J. Appl. Crystallogr.* 45 (2012) 849–854.
- [8] K. Brandenburg, H. Putz, DIAMOND V3.2k (2014), Crystal Impact GbR, Postfach 1251, D-53002 Bonn, Germany.
- [9] H.D. Flack, « On enantiomorph-polarity estimation », *Acta Crystallogr.* A39 (1983) 876-881.
- [10] A.S. Wills, VALIST, V. 1. 5. 8. (1999). CEA, France.
- [11] I.D. Brown, D. Altermatt, « Bond-valence parameters obtained from a systematic analysis of the Inorganic Crystal Structure Database », *Acta Crystallogr.* B41 (1985) 244-247.
- [12] I.D. Brown (1981) in M. O'Keeffe, A. Navrotsky (eds). *Structure and bonding in crystals: II*. Academic Press New York.
- [13] A.A. Udovenko, L.M. Volkova, R.L. Davidovich, L.A. Zemnukhova, E.S. Panin, « Crystal structure of antimony (III) oxyfluoride  $\text{Sb}_3\text{O}_2\text{F}_5$  », *Koord. Khim.* 11 (1985) 1132-1135.

- 
- [14] Sk I. Ali, M. Johnsson, « Antimony oxofluorides – a synthesis concept that yields phase pure samples and single crystals », *Dalton Trans.* 45(30) (2016) 12167-12173.
- [15] K. Holz, R. Mattes, « Verbindungen des Antimon(III) mit  $\text{SbF}_n\text{O}_m$ -Koordinationspähre Kristallstrukturen von  $\text{K}(\text{SbF}_2)\text{HAsO}_4$ ,  $\text{NH}_4(\text{SbF}_2)\text{HAsO}_4$  und  $\text{Sb}_3\text{O}_2\text{F}_5$  », *Z. Anorg. Allg. Chem.* 578 (1989) 133-142.
- [16] A. Aström, S. Andersson, « The crystal structure of L-SbOF », *J. Solid State Chem.* 6 (1973) 191-194.
- [17] A. Aström, « The Crystal Structure of M-SbOF », *Acta Chem. Scand.* 26 (1972) 3849-3854.
- [18] B. Aurivillius, « The Crystal Structure of Bismuth Oxide Fluoride. II. A Refinement of the Previously Published Structure », *Acta Chem. Scand.* 18 (1964) 1823-1830.
- [19] B. Darriet, J. Galy, « Synthèse et structure cristalline du bis[difluorooxostannate(II)] d'étain(II),  $(\text{Sn}_2\text{O}_2\text{F}_4)\text{Sn}_2$  », *Acta Crystallogr.* 33 (1977) 1489-1492.
- [20] I. Abrahams, S.J. Clark, J.D. Donaldson, Z.I. Khan, J.T. Southern, « Hydrolysis of tin(II) fluoride and crystal structure of  $\text{Sn}_4\text{OF}_6$  », *J. Chem. Soc. Dalton Trans.* (1994) 2581-2583.
- [21] J.C. Dewan, A.J. Edwards, « Fluoride crystal structures. Part 27. Seleninyl difluoride at  $-35^\circ\text{C}$  », *J. Chem. Soc. Dalton Trans.* (1976) 2433-2435.
- [22] S.W. Peterson, R.D. Willett, J.L. Huston, « Symmetry and structure of  $\text{XeO}_2\text{F}_2$  by neutron diffraction », *J. Chem. Phys.* 59 (1973) 453-459.
- [23] I. D. Brown, « Bond valence as an aid to understanding the stereochemistry of O and F complexes of Sn(II), Sb(III), Te(IV), I(V) and Xe(VI) », *J. Solid State Chem.* 11 (1974) 214-233.
- [24] D.J. Hodgson, J.A. Ibers, « Crystal and molecular structure of potassium monofluoroxenate(VI),  $\text{KXeO}_3\text{F}$  », *Inorg. Chem.* 8 (1969) 326-331.
- [25] S.E. Ness, D.J.M. Bevan, H.J. Rossell, « Cuboctahedral anion clusters in fluorite-related superstructures. Structure of  $\text{Ca}_2\text{YbF}_7$ , Part 1 », *Eur. J. Solid State Inorg. Chem.* 25 (1988) 509-516.
- [26] S. Kacim, J.C. Champarnaud-Mesjard, B. Frit, « Synthèse et étude cristallographique des phases solides du système  $\text{PbF}_2\text{-InF}_3$  », *Rev. Chim. Miner.* 19(3) (1982) 199-210.
- [27] L. Grosse, R. Hoppe, « Zur Kenntnis von  $\text{Sr}_2\text{RhF}_7$  », *Z. Anorg. Allg. Chem.* 552 (1987) 123-131.

- 
- [28] G. Leinders, R. Delville, J. Pakarinen, T. Cardinaels, K. Binnemans, M. Verwerft, « Assessment of the  $U_3O_7$  Crystal Structure by X-ray and Electron Diffraction », *Inorg. Chem.* 55(19) (2016) 9923-9936.
- [29] B.T.M. Willis, « Positions of the oxygen atoms in  $UO_{2.13}$  », *Nature (London)* 197 (1963) 755-756.
- [30] J.P. Laval, A. Taoudi, A. Abaouz, B. Frit, «  $Lu_3O_2F_5$ : a new highly densified member ( $n = 3$ ) of the  $M_nX_{2n+1}$  series of fluorite-related vernier phases », *J. Solid State Chem.* 119 (1995) 125-130.
- [31] B.G. Hyde, S. Andersson, *Inorganic Crystal Structures*, Eds: Wiley – Interscience, New York (1989).
- [32] D.J.M. Bevan, J. Mohyla, B.F. Hoskins, R.J. Steen, « The crystal structure of some Vernier phases in the Yttrium oxidefluoride system », *Eur. J. Solid State Inorg. Chem.* 27 (1990) 451-465.
- [33] A.J. Edwards, M.A. Mouty, « Fluoride crystal structures. Part V. Potassium pentafluorotellurate(IV) », *J. Chem. Soc. A* (1969) 703-706.

---

**Annexes:**

Table S1: Atomic coordinates ( $\times 10^4$ ) and equivalent isotropic displacement parameters ( $\text{\AA}^2 \times 10^3$ ) for  $\text{Te}_3\text{O}_5\text{F}_2$ .  $U(\text{eq})$  is defined as one third of the trace of the orthogonalized  $U^{ij}$  tensor.

---

	x	y	z	U(eq)
Te(1)	7670(3)	3847(4)	6275(2)	24(1)
Te(2)	9779(3)	937(4)	5764(2)	17(1)
Te(3)	7919(3)	8992(4)	8014(2)	19(1)
Te(4)	4685(3)	2326(4)	8146(2)	17(1)
Te(5)	12584(2)	2858(4)	5557(2)	15(1)
Te(6)	13981(3)	9198(4)	12977(3)	27(1)
Te(7)	5952(3)	9501(4)	5405(2)	22(1)
Te(8)	9658(3)	3164(4)	8904(2)	17(1)
Te(9)	8016(3)	1207(5)	3304(2)	24(1)
Te(10)	8089(3)	3535(4)	9629(2)	18(1)
Te(11)	12076(3)	1417(4)	8743(2)	19(1)
Te(12)	6004(3)	2607(4)	262(2)	18(1)
Te(13)	13885(3)	3110(4)	11555(2)	18(1)
Te(14)	9508(3)	7302(5)	7265(2)	19(1)
Te(15)	14151(3)	9023(4)	6055(3)	27(1)
O(1)	8420(30)	1580(40)	8571(19)	14(5)
O(2)	13980(30)	2070(40)	12700(20)	19(6)
O(3)	12990(30)	4970(40)	11520(20)	17(6)
O(4)	9340(30)	9920(50)	6500(20)	26(7)
O(5)	9150(30)	9120(40)	7910(20)	15(5)
O(6)	14980(30)	4700(40)	12430(20)	19(6)
O(7)	5790(30)	1000(50)	9110(20)	27(7)
O(8)	7260(30)	5070(50)	8690(20)	25(7)
O(9)	15010(30)	500(40)	5850(20)	19(6)
O(10)	8320(30)	6510(50)	6340(20)	24(6)
O(11)	7050(30)	3940(50)	330(20)	24(6)
O(12)	13780(30)	1640(40)	6390(20)	21(6)
O(13)	11550(30)	890(50)	9500(30)	33(8)
O(14)	9140(30)	4740(40)	9530(20)	19(6)
O(15)	6980(30)	5270(40)	6740(20)	15(5)
O(16)	7180(30)	310(50)	6870(20)	25(7)
O(17)	5210(30)	4310(40)	7710(20)	15(5)

---



---

O(18)	6130(30)	2390(50)	5440(20)	24(6)
O(19)	5030(30)	130(50)	4150(20)	26(7)
O(20)	5060(30)	4140(50)	9300(20)	27(7)
O(21)	13020(30)	4750(40)	5000(20)	18(6)
O(22)	13070(30)	40(40)	4960(20)	15(5)
O(23)	9010(30)	4550(50)	7780(20)	24(7)
O(24)	8660(30)	630(50)	4710(20)	25(7)
O(25)	7100(30)	9800(50)	3450(30)	29(7)
F(1)	8400(30)	8240(50)	3200(20)	51(8)
F(2)	10530(30)	5560(50)	9310(20)	49(8)
F(3)	10030(30)	7880(50)	5570(20)	46(7)
F(4)	9290(40)	3640(50)	5950(30)	50(9)
F(5)	12790(30)	3660(40)	9650(20)	34(6)
F(6)	5930(30)	5030(50)	970(20)	42(7)
F(7)	11010(30)	3260(40)	8170(20)	35(6)
F(8)	7110(40)	1190(60)	2020(30)	57(9)
F(9)	7350(40)	3730(60)	3410(30)	64(10)
F(10)	11200(40)	9120(60)	7920(30)	68(11)

---

---

Table S2: Shorter bond lengths [ $\text{\AA}$ ] for  $\text{Te}_3\text{O}_5\text{F}_2$ .

---

Te(1)-O(15)	1.89(3)
Te(1)-O(10)	1.98(3)
Te(1)-O(22)#1	1.99(3)
Te(1)-O(18)	2.43(4)
Te(1)-O(23)	2.48(4)
Te(2)-O(4)#2	1.84(3)
Te(2)-O(24)	1.85(4)
Te(2)-F(4)	1.99(3)
Te(2)-F(3)#2	2.05(3)
Te(3)-O(1)#3	1.88(3)
Te(3)-O(16)#3	1.91(4)
Te(3)-O(3)#4	2.11(3)
Te(3)-O(5)	2.13(3)
Te(4)-O(17)	1.88(3)
Te(4)-O(7)	1.95(4)
Te(4)-O(20)	2.09(3)
Te(4)-O(6)#5	2.13(3)
Te(4)-Te(12)#6	3.170(5)
Te(5)-O(21)	1.88(3)
Te(5)-O(25)#7	1.94(3)
Te(5)-O(12)	1.95(4)
Te(5)-O(22)	2.38(3)
Te(6)-O(2)#3	1.88(3)
Te(6)-O(19)#8	1.99(4)
Te(6)-O(15)#4	2.00(3)
Te(6)-O(17)#4	2.16(2)
Te(7)-O(18)#3	1.86(3)
Te(7)-O(19)#3	1.97(4)
Te(7)-O(21)#1	2.12(3)
Te(7)-O(9)#9	2.13(3)
Te(7)-O(16)#3	2.38(4)
Te(8)-O(23)	1.89(3)
Te(8)-O(14)	1.93(3)
Te(8)-F(2)	1.98(4)
Te(8)-O(1)	2.10(3)
Te(9)-O(25)#2	1.87(4)

---

Te(9)-F(8)	1.96(4)
Te(9)-F(9)	2.00(4)
Te(9)-F(1)#2	2.03(3)
Te(9)-O(24)	2.12(3)
Te(10)-O(8)	1.81(4)
Te(10)-O(13)#4	1.98(3)
Te(10)-O(14)	1.99(3)
Te(10)-O(1)	2.45(2)
Te(11)-O(13)	1.89(3)
Te(11)-F(7)	1.94(4)
Te(11)-F(5)	2.01(3)
Te(11)-F(10)#2	2.06(5)
Te(11)-O(11)#7	2.20(4)
Te(12)-O(11)	1.87(4)
Te(12)-O(20)#10	1.89(4)
Te(12)-F(6)	2.00(3)
Te(12)-O(7)#10	2.08(3)
Te(13)-O(3)	1.87(3)
Te(13)-O(6)	1.98(4)
Te(13)-O(2)	1.98(2)
Te(13)-O(7)#4	2.34(3)
Te(14)-O(5)	1.87(2)
Te(14)-O(10)	1.89(4)
Te(14)-O(4)	2.04(3)
Te(14)-O(23)	2.28(3)
Te(15)-O(9)#3	1.87(3)
Te(15)-O(12)#3	1.95(3)
Te(15)-O(22)#3	1.96(4)
Te(15)-O(6)#11	2.29(3)

Symmetry transformations used to generate equivalent atoms:

#1  $-x+2, y+1/2, -z+1$  #2  $x, y-1, z$  #3  $x, y+1, z$   
#4  $-x+2, y+1/2, -z+2$  #5  $-x+2, y-1/2, -z+2$  #6  $x, y, z+1$   
#7  $-x+2, y-1/2, -z+1$  #8  $x+1, y+1, z+1$  #9  $x-1, y+1, z$   
#10  $x, y, z-1$  #11  $-x+3, y+1/2, -z+2$  #12  $-x+3, y-1/2, -z+2$   
#13  $x+1, y-1, z$  #14  $x-1, y-1, z-1$

Table S3 : Anisotropic displacement parameters ( $\text{\AA}^2 \times 10^3$ ) for  $\text{Te}_3\text{O}_5\text{F}_2$ . The anisotropic displacement factor exponent takes the form:  $-2\pi^2[ h^2 a^{*2} U^{11} + \dots + 2 h k a^* b^* U^{12} ]$

	$U^{11}$	$U^{22}$	$U^{33}$	$U^{23}$	$U^{13}$	$U^{12}$
Te(1)	36(3)	19(1)	30(2)	9(1)	25(3)	12(2)
Te(2)	11(3)	19(1)	17(2)	1(1)	3(2)	-2(2)
Te(3)	22(3)	16(1)	20(2)	0(1)	12(2)	-1(2)
Te(4)	13(3)	18(1)	19(2)	2(1)	7(2)	1(2)
Te(5)	12(3)	16(1)	14(1)	-1(1)	4(2)	0(1)
Te(6)	25(3)	13(1)	50(2)	-1(2)	25(3)	-1(2)
Te(7)	24(3)	13(1)	35(2)	0(1)	21(3)	-1(2)
Te(8)	14(3)	21(1)	15(1)	2(1)	5(2)	2(2)
Te(9)	24(3)	28(2)	19(2)	6(1)	10(2)	-5(2)
Te(10)	17(3)	19(1)	15(2)	2(1)	5(2)	1(2)
Te(11)	13(3)	23(1)	17(2)	3(1)	4(2)	-1(2)
Te(12)	13(3)	24(1)	14(1)	-5(1)	6(2)	-3(2)
Te(13)	13(3)	26(1)	12(1)	-3(1)	3(2)	2(2)
Te(14)	10(3)	31(2)	13(1)	-1(1)	2(2)	6(2)
Te(15)	23(3)	17(1)	49(2)	11(2)	24(3)	7(2)

•**Te<sub>3</sub>O<sub>5</sub>F<sub>2</sub>**: a new metastable tellurium IV oxyfluoride with an acentric complex structure

•Jean-Paul Laval\*, N. Jennene-Boukharrata and Philippe Thomas

Centre Européen de la Céramique,  
IRCER, UMR-CNRS 7315, Université  
de Limoges, Faculté des Sciences,  
12 rue Atlantis, 87068 Limoges, France.

The crystal structure of Te<sub>3</sub>O<sub>5</sub>F<sub>2</sub> is unusually complex with 15 different Te polyhedra. It is built of giant cylindrical columns of oxide units connected *via* weak Te-F bonds. A strict O/F order is evidenced. It derives from anion-excess fluorite type.

